Implementing the Results of Ventilation Research
16th AIVC Conference, Palm Springs, USA
19-22 September, 1995

High Resolution Particle-Imaging Velocimetry for Full-Scale Indoor Air Flows

M M Cui*, C Topp**, S Pedersen**, L L Christianson*, R J Adrian*, K W Leovic***

* Bioenvironmental Engineering Research Lab., University of Illinois at Urbana-Champaign, Urbana, Ill 61801, USA
** Dept of Building Technology and Structural Engineering, Aalborg University, Sohngaardsholmsvej 57, 9000 Aalborg, Denmark
*** Indoor Air Branch (MD-54), Air and Energy Engineering Research Lab., U S Environmental Protection Agency, Research Triangle Park, NC 27711, USA

ABSTRACT

A high resolution particle-imaging velocimetry has been developed and applied to study full-scale room air flows. The system is designed to study local field quantities in occupied zones (microclimate), ventilation effectiveness, and airborne pollutant transport in the indoor environment. The system can be applied to evaluate indoor environment in typical commercial and residential settings. The technique and instrumentation have been applied successfully to study localized air flow patterns and particle concentration distribution in the indoor environment. The results of this research can be used to assess the ventilation effectiveness and energy effeciecy in rooms and buildins.

INTRODUCTION

To maintain comfort and suitable indoor air quality within occupied zones of a building, conditioned outdoor air usually is introduced by a heating, ventilating, and air-conditioning (HVAC) system. Due to different arrangements of rooms and of diffusers and returns, different air flow patterns can be obtained in rooms (Figures 1, 2, and 3). Improper air distribution patterns not only reduce ventilation effectiveness but also cause occupant discomfort even when the overall ventilation rate is sufficient. In fact, most complaints by the building occupants about discomfort are associated with non-uniformity of air temperature, large velocity gradients (air drafts), and localized microclimates in occupied spaces[1]. The room air distribution greatly affects the distribution and transport of airborne pollutants in buildings and rooms and occupant exposure to these pollutants. In many cases, emission rates of particulate and gaseous air pollutants depend on the air flow patterns near the pollutant sources (e.g., product usage, building materials, furniture, and occupants). To best address these issues, the microstructure of indoor air distribution is being studied.

In the present study, a high resolution particle-imaging velocimetry has been developed. This system consists of three sub-systems which illuminate flow structures, acquire images, and interrogate these images to obtain the velocity and particle concentration distribution.

ILLUMINATION

The illumination system is the starting point of this research. The basic function of this system is to visualize the flow patterns and/or particles. These visualized flow and particle movements can be recorded and processed. Since the light energy per unit area is inversely proportional to the total area illuminated, illumination of a full-scale room is one of the most important parts of this research. To obtain uniformity of illumination over a large space, four halogen lamps are used. The light is controlled by four cylindrical lenses installed in front of the light bulbs. Lens focal length is 90 mm. The depth of the field, δz, is calculated as[2]:

$$\delta z = 4(1+M)^2 f^{\#2} \lambda, \tag{1}$$

where M is the camera magnification, $f^{\#}$ is the camera f-number, and λ is the wave length of the illumination light. The cylindrical lens used actually changes the point light source to a line light source. To maximize light intensity, the minimum value of the f-number (maximum aperture) is used in the experiments. The thickness of the light sheet is chosen as the depth of field to minimize the background noise caused by light scattered by the particles out of the depth of field. To reduce the light scattering from the space around the lens, the lamps are placed in an air-cooled cabinet which is sealed so that light comes out only through a thin slot. Each of the four lamps consists of an aluminum chassis with a 1,500 W bulb. Bulbs are cylindrical and behave like a line source. The light sheet generated is 50 mm thick across the test room. The thickness of the light sheet is uniform.

In the present study two types of particles are used. The first type are neutrally buoyant, helium-filled bubbles 1 mm in diameter. Since these bubbles behave as a low pass filter, the flow structure is obtained only when this structure is larger than 1 mm. Flow structures smaller than 1 mm are obtained as averaged effects. The helium in the bubbles is kept at the same temperature as the room air. Bubbles are seeded uniformly in the test room and they follow flows well. Plastic microspheres are the second type of particles. These particles are heavier than air. The size distribution is from 10 to 100 µm. Tests on aerosol and dust particles with different sizes are in progress.

Since the large room size (2.53 by 3.60 by 2.43 m) requires a strong illuminating light source to make small particles visible, the parameters need to be optimized to ensure image quality. Mean exposure ($\bar{\varepsilon}$) averaged over the area of a particle image is given by[2]:

$$\bar{\varepsilon} = \frac{\lambda^2 W \int |\sigma| \, d\Omega}{\pi^3 [M^2 d_p^2 + 2.44^2 (1+M)^2 f^{\#2} \lambda] \Delta y_0 \Delta z_0}, \tag{2}$$

$$\sim \frac{\lambda^2 W d_p^n D_a^2}{\lambda^n d_o^2 (M^2 d_p^2 + 2.44^2 d_i^2 \lambda^2 / D_a^2) \Delta y_0 \Delta z_0}, \tag{3}$$

where W is the energy of the light pulse, σ is the Mie scattering coefficient of the particle, Ω is the solid angle, D_a is the lens aperture diameter, and n is the power-law exponent describing the scattered light energy. In our case, W is the light energy transmitted to the film each time the camera shutter is opened. As particle size increases into the geometric scattering regime, the equation becomes:

$$\bar{\varepsilon} \propto \frac{W D_a^2}{d_0^2 M^2 \Delta y_0 \Delta z_0}, \tag{4}$$

which implies that light intensity, shutter speed, and lens aperture diameter control film mean exposure.

IMAGE ACQUISITION

Although the designed resolution of the system is 1 mm, the system needs to acquire high quality images of the helium-filled bubbles with 1 mm diameter. Therefore, much higher resolution is needed for particle images. If the film used has a resolution of 320 line pairs per mm (Kodak Technical Pan film) and one line pair is needed to resolve 1 mm, the film size needed is about 6 by 4 mm for a view area of 2,000 by 1,500 mm. Actually, more than one line pair are needed to obtain a high quality image of 1 mm size. The film size (36 by 24 mm) used in this research is much larger than the calculated minimum size. With the frame size of 36 by 24 mm, the camera can provide six line pairs per mm for the size of the given objective field to obtain circular bubble images.

Shutter speed, characterized by the opening time, δt, and time interval between the exposures, Δt, are the critical parameters for the image acquisition in the tests. The former is a measure of the distance particles travel when the shutter is open causing the elongated image. The latter is a measure of the distance particles travel between two sequential openings of the camera shutter, which determines the distance between particle images on the film. To obtain the best results, Δt is bounded by the optimized displacement of particle images (3 to 5 particle image diameters). The ratio $\Delta x / \delta x$ is chosen as 10 in current experiments. Therefore, the displacement of particles is $0.3 d_p$ for maximum velocity in the room, where d_p is particle image diameter.

Since room flows have large inverse velocities, image-shift techniques are used to determine the direction of velocity. Shift velocity is calibrated, using both stationary images and measurement of shift velocity. Velocity of the shift (U_s) is determined by camera magnification (M) and the maximum flow velocity in the opposite direction of the shift (u_{max}). Based on the measurement of air jet velocity (0.9 m/s) near the diffuser and analysis of some test images, the minimum speed of the shift has been determined. The camera is shifted by a stepmotor which moves at a constant speed of 0.2 m/s.

When the camera shutter opens, intensity $I_{oi}(x)$; $i = 1, 2, \ldots, n$, produces a multiple-exposed single photographic film with particle images. Each of these intensities is separated by a time interval, Δt, from a constantly illuminated light sheet of thickness, Δz. Simultaneous in-plane velocity measurements can be obtained from these images.

A sample image is shown in Figure 4. The image has been shifted to the left to solve direction ambiguity. The distribution of the bubbles is uniform and the density is high. To increase the strength of the signal, quadruple exposures are used.

Concentration has been measured using a Charge-Coupled Device (CCD) camera. Since the light intensity scattered by the particles is proportional to their concentration, the camera is not required to resolve individual particles, although it is the ultimate goal of the measurement.

INTERROGATION

The images acquired are interrogated to obtain the information needed. For velocity measurements, the images were processed by a computer system for Particle-Imaging Velocimetry (PIV)[3]. An analog image signal is sent from a CCD camera to the frame grabber, where it is digitized and stored as a 1024 by 1024 pixel image. Then the digitized image is divided into eight sub-images and processed in two array processor boards (MC860VS) each with four i860 microprocessors.

When a multiple-exposed photograph is interrogated by a light beam of intensity $I_I(\mathbf{X}-\mathbf{X}_I)$, centered at $\mathbf{X}_I$, the transmitted light intensity after the photograph is:

$$I(\mathbf{X}) = I_I(\mathbf{X}-\mathbf{X}_I)\tau(\mathbf{X}), \tag{5}$$

where $\tau(\mathbf{X})$, the intensity transmissivity of the photograph for multiple exposures equally spaced in time, is:

$$\tau(\mathbf{X}) = \sum_i \sum_{j=1}^{n} I_{oj}\tau_o[\mathbf{X} - M\mathbf{x}_i(t + (j-1)\Delta t)]. \tag{6}$$

The spatial autocorrelation of $I(\mathbf{X})$ with separation $\mathbf{s}$ is approximated by the spatial average over the interrogation spot:

$$R(\mathbf{s}) = \int I(\mathbf{X})I(\mathbf{X}+\mathbf{s})d\mathbf{X}. \tag{7}$$

It consists of five components[4]:

$$R(\mathbf{s}) = R_C(\mathbf{s}) + R_P(\mathbf{s}) + R_{D^+}(\mathbf{s}) + R_{D^-} + R_F(\mathbf{s}), \tag{8}$$

where R_{D^+} is the correlation of all earlier images shifted by $\mathbf{s}$ with subsequent unshifted images, while R_{D^-} is the correlation of all later images shifted by $\mathbf{s}$ with prior unshifted images. Both R_{D^+} and R_{D^-} can be decomposed further when the pulse separation is constant:

$$R_{D^+} = R_{D^+}^{(1)} + R_{D^+}^{(2)} + \cdots + R_{D^+}^{(n-1)}, \tag{9}$$

where $R_{D^+}^{(k)}(\mathbf{s})$ is the correlation of all earlier images shifted by $\mathbf{s}$ with subsequent unshifted images at a later time separation, $k\Delta t$[5]. A similar decomposition exists for $R_{D^-}^{(1)}(\mathbf{s})$.

To determine the mean image displacement across the interrogation spot between successive pulses, the centroid of $R_{D^+}^{(1)}(\mathbf{s})$ is located by:

$$\mu_D^{(1)} = \frac{\int \mathbf{s}R_D^{(1)}(\mathbf{s})d\mathbf{s}}{\int R_D^{(1)}(\mathbf{s})d\mathbf{s}}. \tag{10}$$

If the successive pulse intervals are equal to Δt, the measured in-plane velocity is calculated as:

$$\mathbf{u}(\mathbf{x}_l) = \frac{\mu_D^{(1)}}{M\Delta t}. \tag{11}$$

For concentration measurements, the particle concentration distribution is calculated from the number of the particles per unit volume:

$$C = \frac{n}{V}. \tag{12}$$

TEST ROOM AND PROCEDURE

The Room Ventilation Simulator (RVS) at UIUC is used to study air and air contaminant distributions within ventilated rooms[6]. The RVS consists of an adjustable inner room and an outer room for controlling ambient environmental conditions of the inner test room. The outer room of the RVS (Figure 5) is an insulated, 12 by 9 by 3.6 m building used to simulate climatic conditions ranging from cold winter to hot summer around the inner test room. The outer room HVAC system, which includes an air cooling condenser, compressors, an evaporator, electric heaters, a supply fan, and a control system, is designed to provide temperatures raging from -27 to 40°C. The inner room of the RVS is modular so that different room configurations and sizes (up to 10 by 7 by 3 m) can be modeled conveniently. Cold or warm air can enter the inner test room directly from the outer room. Alternatively, the independent HVAC system for the inner room provides constantly conditioned supply air (ranging from -27 to 40°C) for the inner test room. At the same time, conditions around the inner test room can be maintained at a different temperature.

A test room, 2.53 by 3.60 by 2.43 m, has been constructed inside the RVS. The front and the left sides of the test room are clear, tempered glass to permit optical access to the interior of the room. The other two walls are wood and painted black to obtain a perfect optical environment (Figures 6 and 7). The test room has been designed and constructed to make it easy to change configurations of the room, such as the locations of the diffusers and air returns, furniture, carpet, and occupants (models or real people). The test room is supplied with air through a closed-loop fan system. A configuration with both a linear diffuser and a linear exhaust has been designed and constructed. Four supply tubes connect the high pressure side of the fan to a diffuser box mounted on top of the test room, and the exhaust is connected to the low pressure side via a sealed room next to the test room. Figure 8 outlines the diffuser box and the positions of supply tubes. Each of the supply tubes has a damper for individual control of air flow. A porous screen is mounted inside the diffuser box to make the outgoing velocity profile uniform (Figure 9). The damper positions are adjusted to ensure a uniform velocity. Velocity profiles for different damper positions are shown in Figure 10.

The HVAC system is turned on for 30 minutes for each air change rate to ensure that the room air flow reaches a steady state. The light is switched on only during image acquisition, which only takes 0.5 min. If a large number of frames are needed for statistical analysis, the process is split into a few short sessions. Room temperature is maintained at 21±0.5°C (70±0.9°F) throughout the tests.

RESULTS AND DISCUSSIONS

Experiments have been conducted with air change rates of 5 and 10 air changes per hour (ACH). Figure 11 shows the size and position of the objective plan in the test room at 5 ACH. Figure 12 shows the correspondent velocity distribution for 5 ACH, and Figures 13 and 14 show the objective plan and velocity distribution for 10 ACH. For 10 ACH, the camera was placed closer to the objective plan which then gave a smaller view field and a lower relative bubble density.

Depending on the structures of room air flows and seeding particle density, 2,000 to 8,000 vectors can be obtained for the size of the given two-dimensional space. The small scale structures of air flows can be seen clearly in Figures 12 and 14. This capability is critical for the study of diffusion effect dominated by small structures in the indoor environment, which in turn is important for particle transport.

The results also show that the air flows in most parts of the room are slower than 0.1 m/s at a normal range of air change rates (~ 3 to 10 ACH). There is no instrumentation commercially available to measure slow velocity in this region. The capability to measure such low velocities gives the described system another unique feature which will be useful in helping aerosol manufactures and other industries to improve their products.

A contour plot of particle concentration with 5 ACH is shown in Figure 15. Although the concentration distribution of the particles appears to be complicated, the particles are denser in the lower part of the room and more dilute in the upper part of the room.

CONCLUSIONS

A non-intrusive, whole-field measurement technique for studying indoor air quality has been developed. Two-dimensional structures of full-scale room air flows and particle concentration have been determined. The technique shows great potential for helping us to understand ventilation effectiveness and indoor air quality since mixing efficiency, fresh air delivery rate to occupied zone, and transport of particulate air pollutants can be calculated from instantaneous velocity and concentration distribution. It also can serve as a bench mark test for global measurement techniques, such as tracer gas techniques, and computational fluid mechanics models.

ACKNOWLEDGEMENTS

This work is partially supported by the U.S. EPA's Office of Research and Development's National Risk Management Research Laboratory. The authors would also like to thank Paul L. Miller of the National Renewable Energy Laboratory for his helpful suggestions and comments on the design of the test room.

REFERENCES

1. Hansen, S. J.; *Managing Indoor Air Quality;* The Fairmont Press, Inc.: Lilburn, GA, 1991; pp 81-113.
2. Adrian, R. J.; Annual Review of Fluid Mechanics **1991** 23, 261-304.
3. Meinhart, C. D.; Prasad, A. K.; Adrian R. J.; Measurement Science and Technology **1993** 4, 619-626.
4. Adrian, R. J.; Laser Anemometry in Fluid Mechanics **1988** 3, 115-129.
5. Keane, R. D.; Adrian, R. J.; Measurement Science and Technology **1991** 2, 1202-1215.
6. Wu, G. J.; Christianson, L. L.; Zhang, J. S.; Riskowski, G. L.; "Adjustable Room Ventilation Simulator for Room Air and Air Contaminant Distribution Modelling," in *Proceedings of the Fifth International Conference on Indoor Air Quality and Climate*, 1990, pp. 237-242.

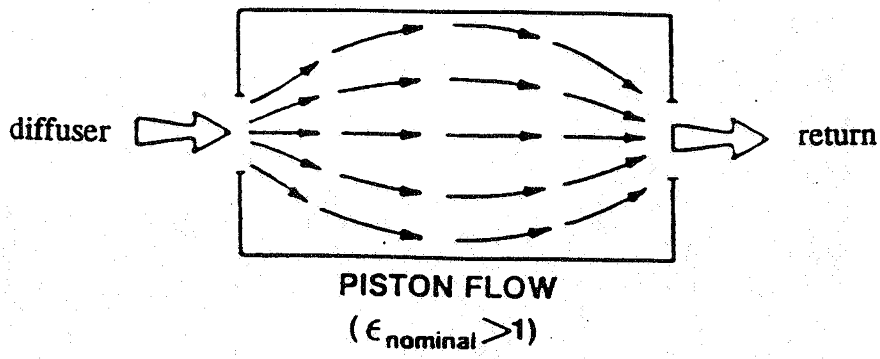

Figure 1. Piston flow. (Source: U.S. Department of Energy.)

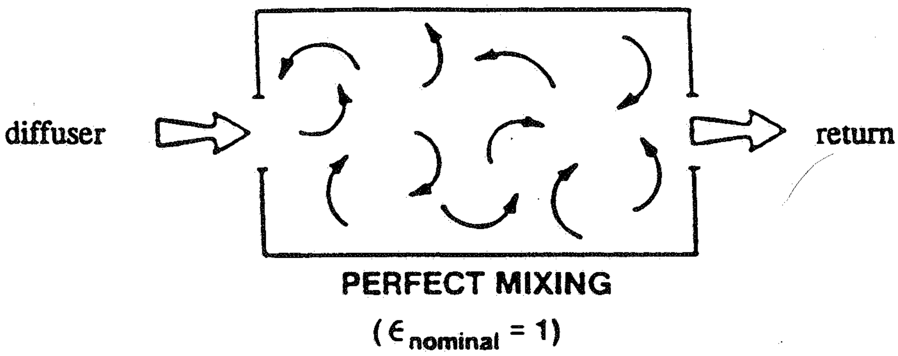

Figure 2. Perfect mixing. (Source: U.S. Department of Energy.)

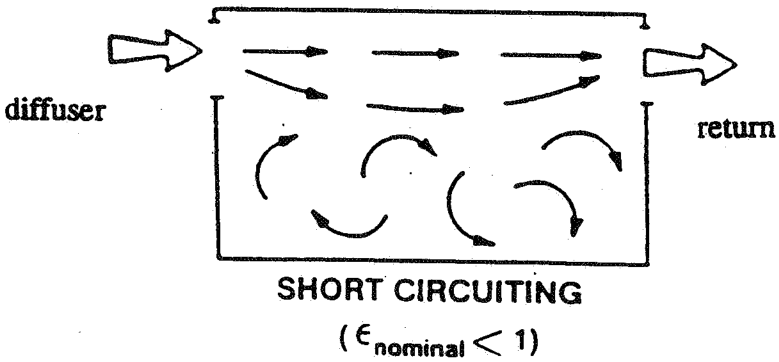

Figure 3. Short circuiting. (Source: U.S. Department of Energy.)

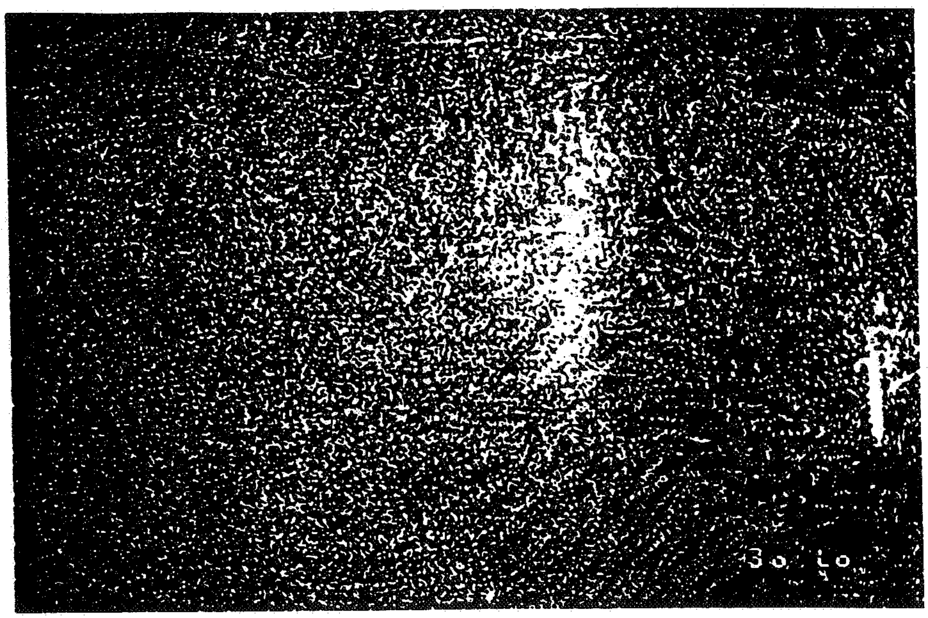

Figure 4. Room air flow with bubbles. (Air change rate = 5 ACH.)

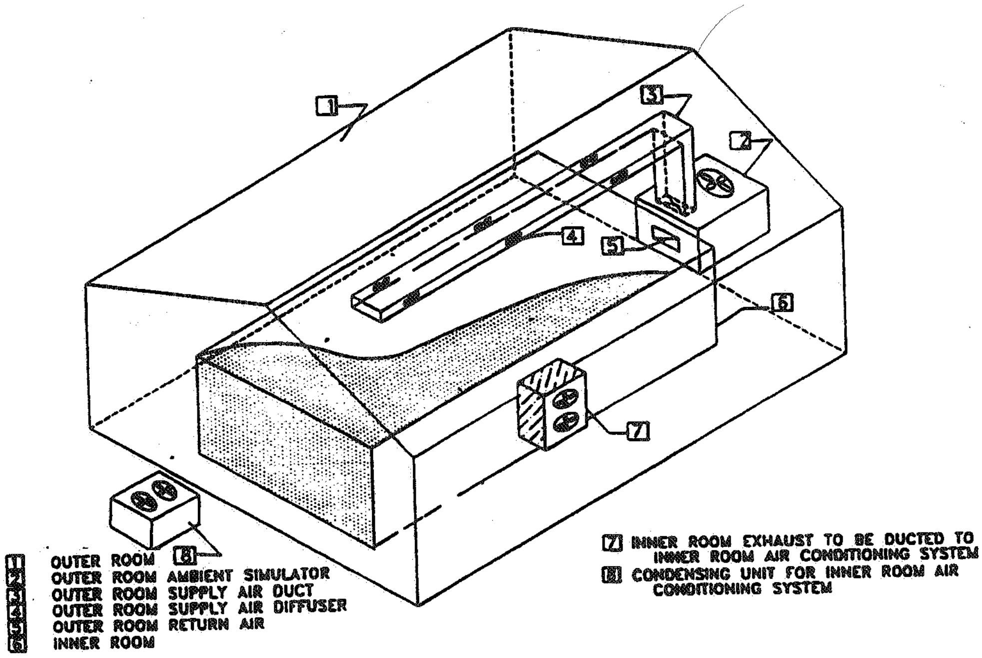

Figure 5. Room Ventilation Simulator.

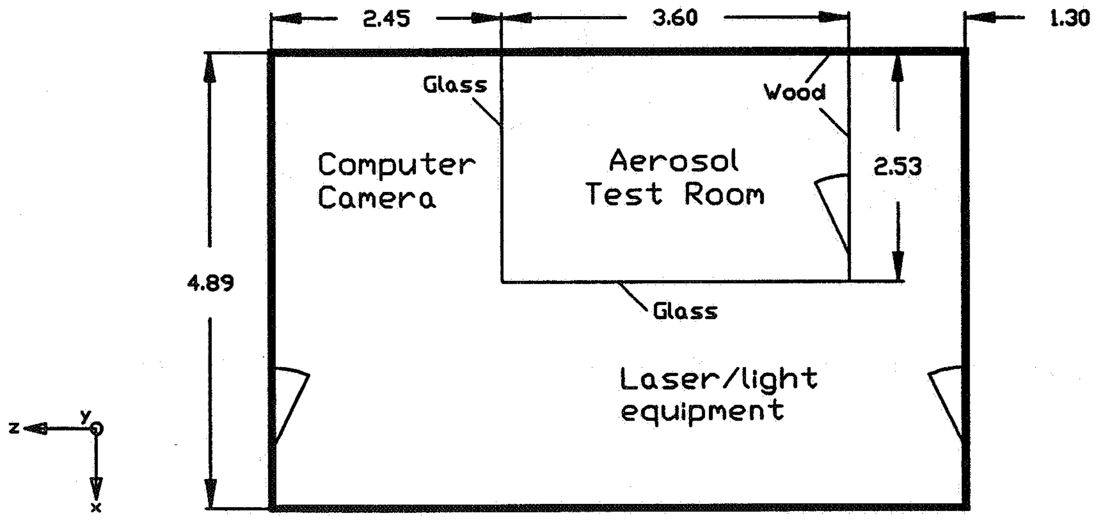

Figure 6. Plan drawing of the inner room and the test room. (All dimensions in meters.)

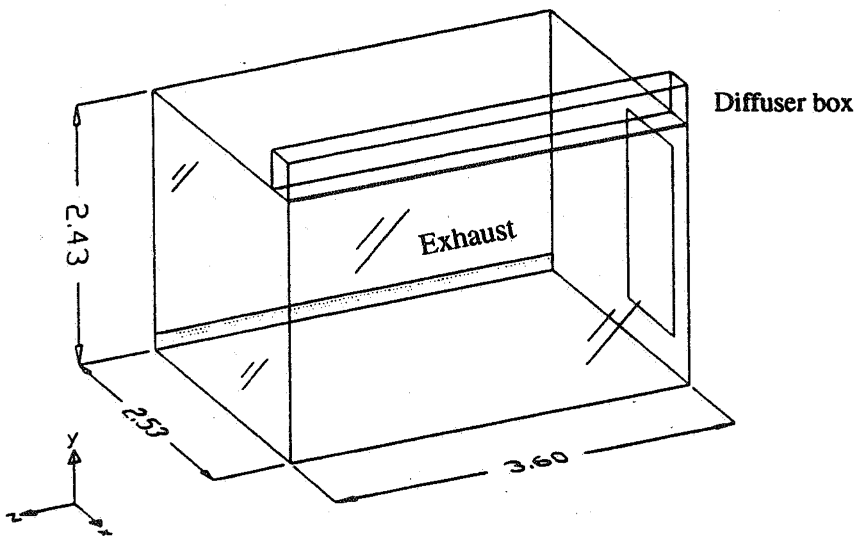

Figure 7. Dimensions and configuration of the test room. (All dimensions in meters.)

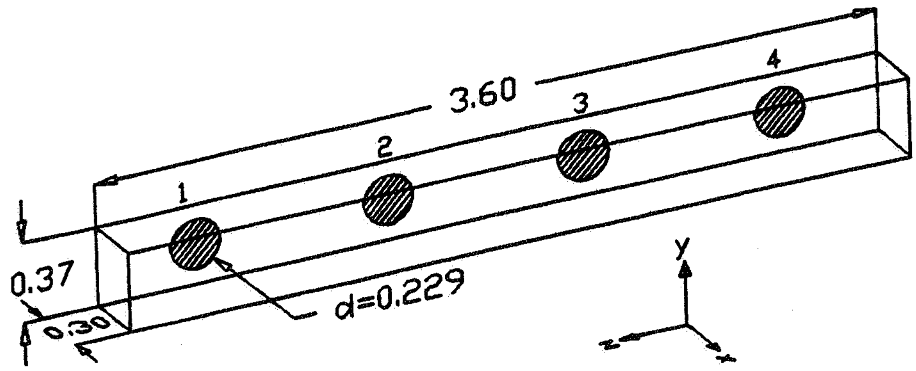

Figure 8. Diffuser box for providing the room with a two-dimensional air flow. (All dimensions in meters.)

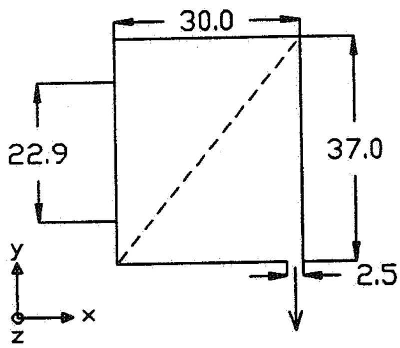

Figure 9. Cross-section of diffuser box. (All dimensions in centimeters.)

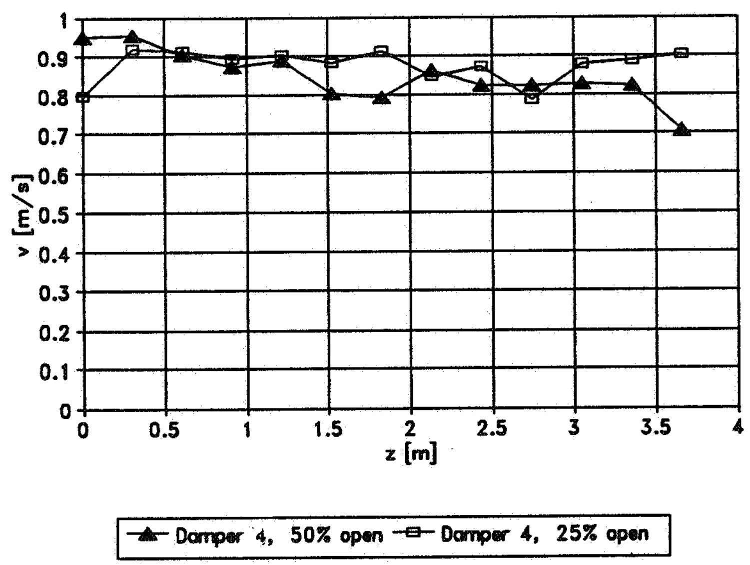

Figure 10. Inlet velocity profiles along the z-axis for two positions of the left damper.

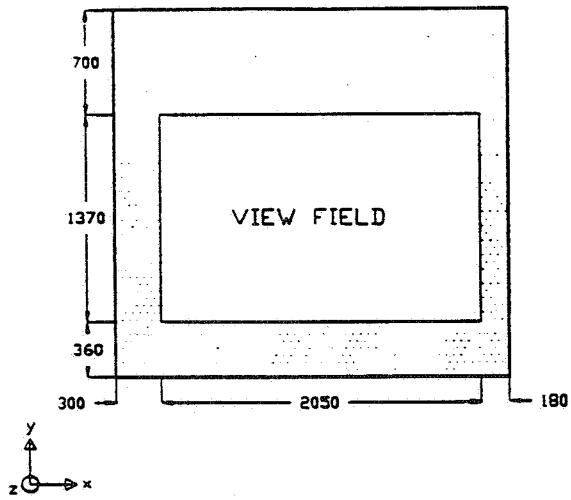

Figure 11. Size and position of the objective plan in the test room for air change rate = 5 ACH. (All dimensions in millimeters.)

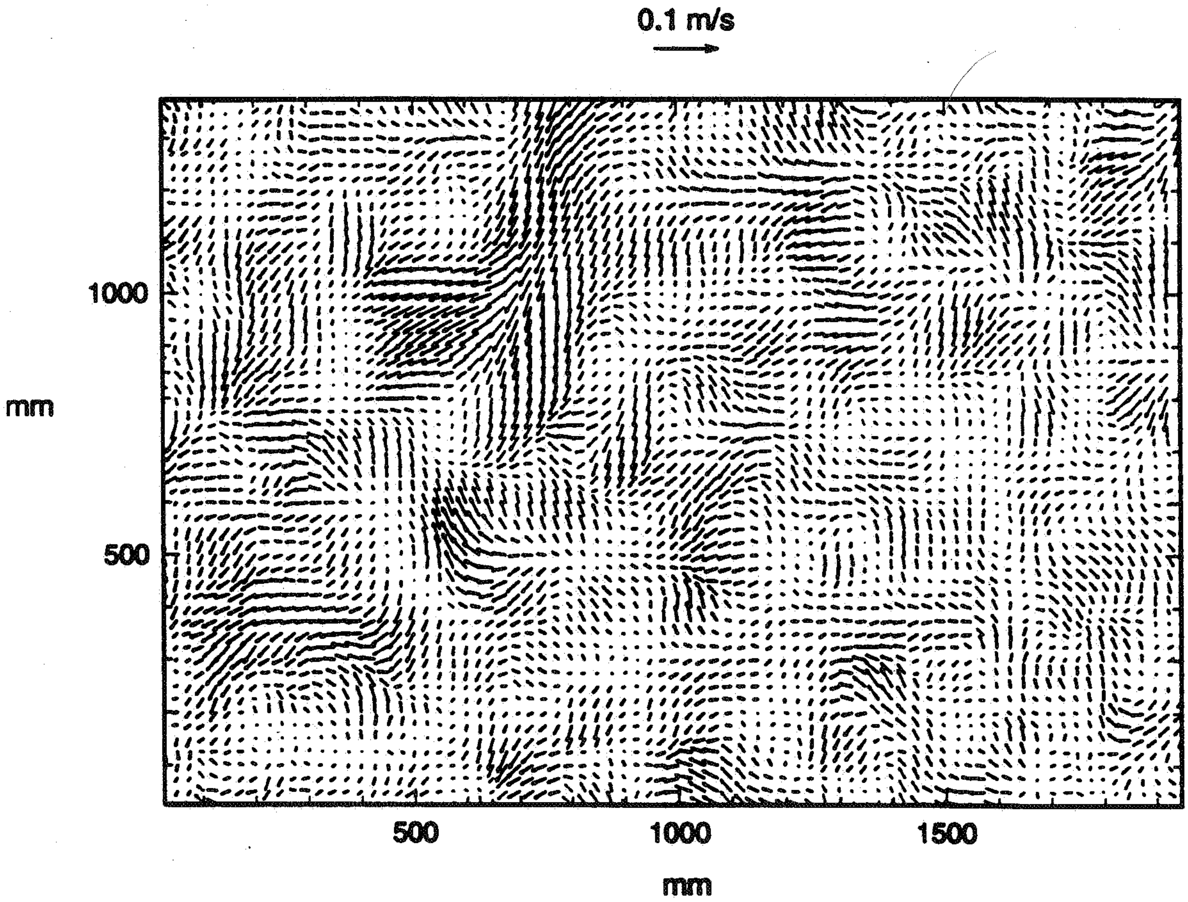

Figure 12. Vector map of room air flow for air change rate = 5 ACH.

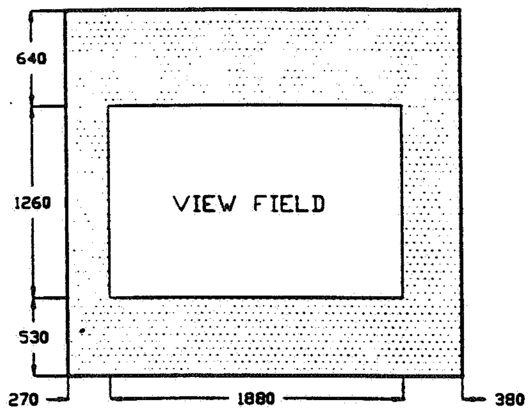

Figure 13. Size and position of the objective plan in the test room for air change rate = 10 ACH. (All dimensions in millimeters.)

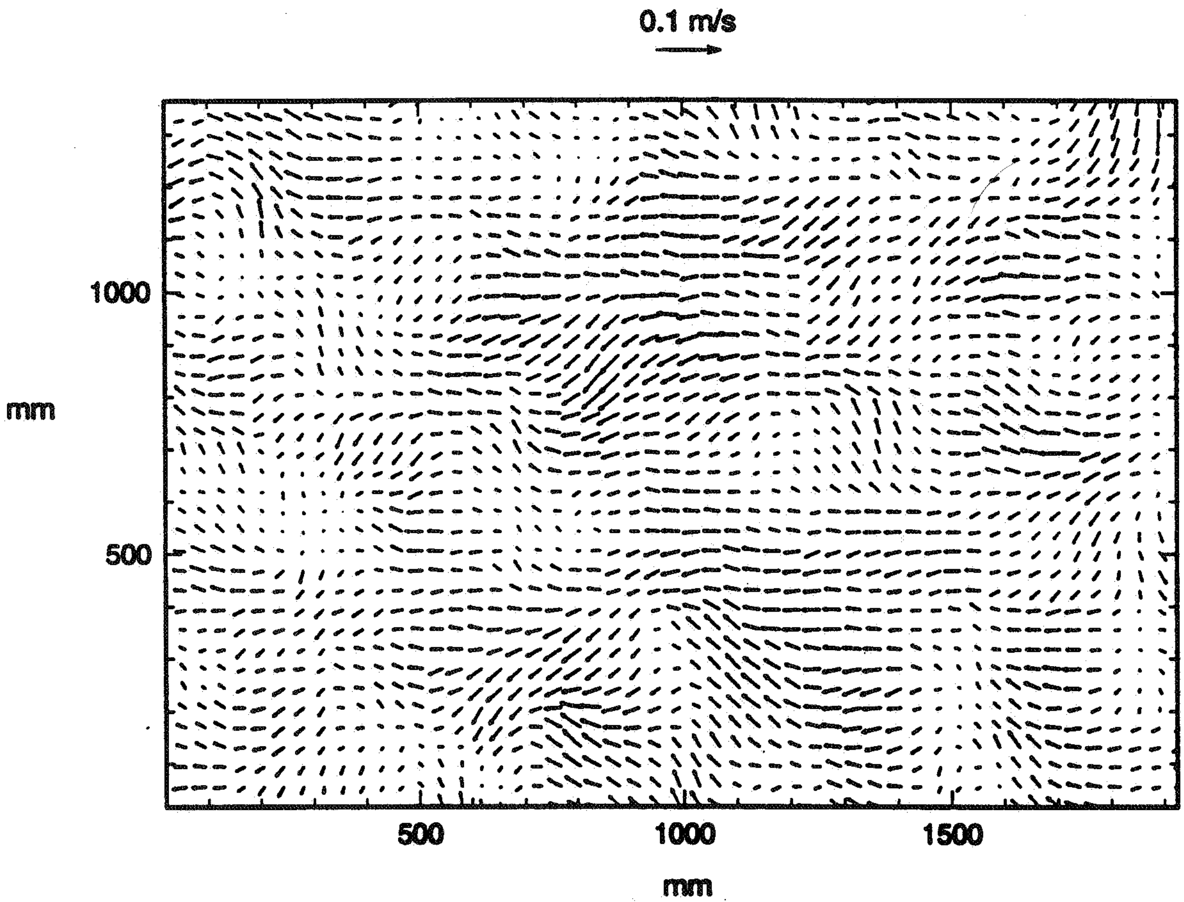

Figure 14. Vector map of room air flow for air change rate = 10 ACH.

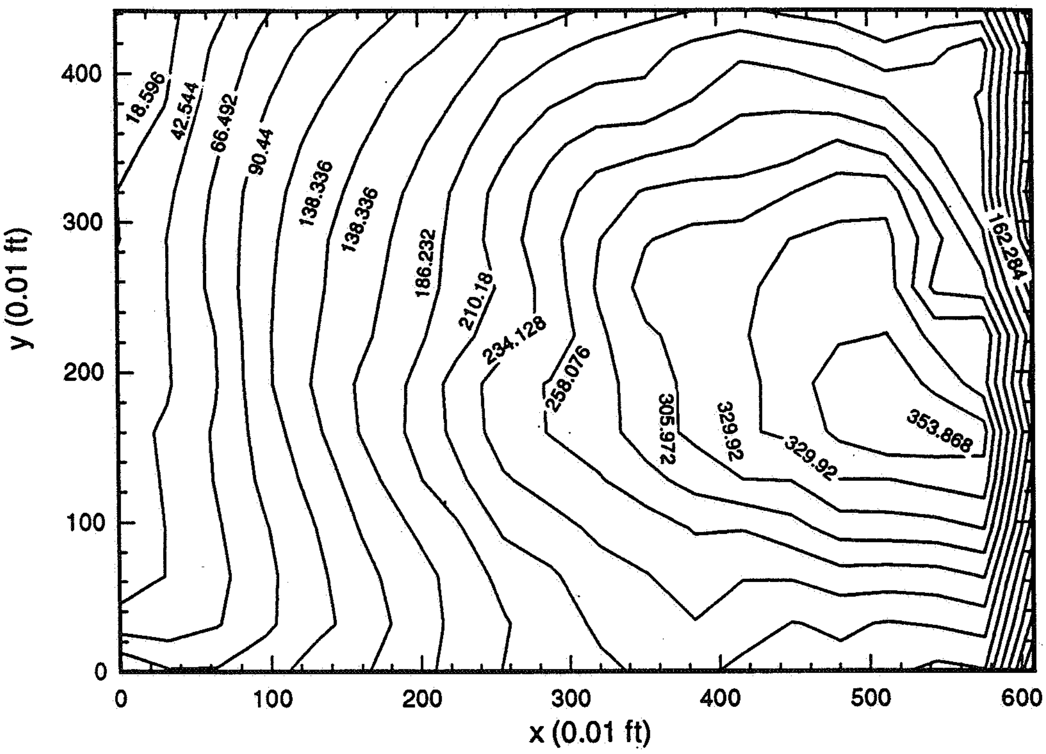

Figure 15. Contour plot of particle concentration distribution in cubic feet (×1000) for air change rate = 5 ACH.